Density-functional-theory response-property calculations with accurate exchange-correlation potentials

S. J. A. van Gisbergen,[1] F. Kootstra,[2] P. R. T. Schipper,[1] O. V. Gritsenko,[1] J. G. Snijders,[2] and E. J. Baerends[1]
[1]*Department of Physical and Theoretical Chemistry, Vrije Universiteit, De Boelelaan 1083, 1081 HV, Amsterdam, The Netherlands*
[2]*Department of Chemical Physics and Materials Science Centre, Rijksuniversiteit Groningen, Nijenborgh 4, 9747 AG Groningen, The Netherlands*
(Received 6 November 1997)

Response calculations in the framework of time-dependent density-functional theory (TDDFT) have by now been shown to surpass time-dependent Hartree-Fock (TDHF) calculations in both accuracy and efficiency. This makes TDDFT an important tool for the calculation of frequency-dependent (hyper)polarizabilities, excitation energies, and related properties of medium-sized and large molecules. Two separate approximations are made in the linear DFT response calculations. The first approximation concerns the exchange-correlation (xc) potential, which determines the form of the Kohn-Sham orbitals and their one-electron energies, while the second approximation involves the so-called xc kernel f_{xc}, which determines the xc contribution to the frequency-dependent screening. By performing calculations on small systems with accurate xc potentials, constructed from *ab initio* densities, we can test the relative importance of the two approximations for different properties and systems, thus showing what kind of improvement can be expected from future, more refined, approximations to these xc functionals. We find that in most, but not all, cases, improvements to v_{xc} seem more desirable than improvements to f_{xc}. [S1050-2947(98)10004-5]

PACS number(s): 31.15.Ew, 33.15.Kr

I. INTRODUCTION

Several reliable quantum-chemical *ab initio* methods have become available over recent years for the accurate determination of such molecular properties as excitation energies, frequency-dependent polarizabilities, and frequency-dependent hyperpolarizabilities. In particular, we mention coupled-cluster response theory [1,2], multiconfiguration time-dependent Hartree-Fock (MCTDHF) [3], and time-dependent MP2 [4–7], which have, among other things, been used for the calculation of hyperpolarizabilities and excitation energies.

However, because they are computationally intensive, these methods are restricted to small or medium-sized systems. For systems where the cost of the most reliable of these *ab initio* methods becomes prohibitive, a computationally more efficient method is required, which is accurate at the same time. Density-functional theory (DFT) provides such a method through its time-dependent extension (TDDFT).

Almost two decades ago, Zangwill and Soven [8] were among the first to apply this theory in the linear response regime. They calculated photoabsorption cross sections of rare gases in the local density approximation (LDA). Only a few years later did the rigorous justification of their approach appear, with the work of Runge and Gross [9], who proposed a set of time-dependent Kohn-Sham (KS) equations. For a recent review of TDDFT and applications of it, the reader is referred to Ref. [10].

The first response calculations on molecules in this framework appeared only recently (after an initial attempt by Levine and Soven, [11] whose approach was based on a single-center expansion which made it impractical for general molecules). At the moment several groups have performed (molecular) response calculations using TDDFT. Calculations on frequency-dependent multipole polarizabilities [12–15], excitation energies [16–19,13,20–23], frequency-dependent hyperpolarizabilities [24], Van der Waals dispersion coefficients [25,14], and Raman scattering [26] have appeared until now. From the data in these papers it appears that the TDDFT results are usually superior to their TDHF counterparts, and in many cases competitive with correlated *ab initio* results at the TDMP2 level. At the same time, implementations of the TDDFT linear response equations using auxiliary basis functions (fit functions) [25,20,22] have been reported to scale as N^3 (N being the number of atoms in the calculation), which is even more favorable than the nominal N^4 scaling of TDHF. TDDFT thus surpasses TDHF both in the accuracy of the results and in the efficiency of the calculations.

Now that the usefulness of TDDFT in this regime has been firmly established and many different properties can be routinely obtained, it is of importance to know which factors restrict the accuracy of the TDDFT calculations. If an even higher quality in the results is required than is attainable with the approximations that are presently used in these calculations, it will be important to know which approximations have the largest influence on the various properties that are accessible.

Apart from practical limitations in accuracy due to the use of finite basis sets, two approximations are made in the TDDFT linear-response calculations: one for the usual xc potential v_{xc} and one for the less common xc kernel f_{xc}. Our aim is to estimate the importance of the two approximations by performing calculations using accurate xc potentials constructed from essentially exact *ab initio* densities. If such a density is available, one can construct an xc potential which yields this target density, by iteratively adapting the xc potential until the target density is finally obtained within sat-

isfactory accuracy, in a KS calculation with this potential. In this manner, the approximation for v_{xc} is basically removed. By increasing the technical accuracy of the calculations to the limit (we are referring to basis and fit set size, integration accuracy, convergence criterion for the iterative solution of the KS equations, and so on), we can be sure that the bulk of the remaining deviations from the experimental values is due to deficiencies in the second approximation: the approximation to f_{xc}.

Unfortunately, the reliable xc potentials which are needed for these calculations are available for a few small systems only: the He, Be, and Ne atoms. The reason for this is that virtually all accurate densities are obtained from *ab initio* programs using Gaussian-type orbitals (GTOs). Constructing an xc potential belonging to such a density leads to certain anomalies in the potential which are due to the specific properties of the GTOs. The anomalies include an incorrect asymptotic behavior and spurious oscillations in the potential [27]. The exact xc potential should asymptotically display a $-1/r$ behavior, but a Gaussian density results in a potential which diverges quadratically at infinity. Furthermore, the potential exhibits oscillations which are also due to the use of Gaussian basis functions. Although these oscillations should disappear in the basis-set limit, they form a practical problem even for very large GTO basis sets.

This problem can be circumvented by using accurate densities based on Slater-type orbitals (STOs) or densities which have not been expanded in a basis set at all. Such densities, however, are rare. Accurate densities based on STOs are, to the best of our knowledge, only available for Be and Ne. These densities were obtained by Bunge and Esquivel from a CI calculation using large STO basis sets [28,29]. For He and Be, accurate xc potentials have been constructed by Umrigar and Gonze [30,31]. They numerically generated essentially exact densities for these systems by integrating very accurate wave functions [30] (for He) or by employing various Monte Carlo techniques [31] (for Be).

For these atomic systems, we have calculated several response properties, such as static dipole and quadrupole polarizabilities, the frequency dependence of the dipole polarizability, singlet and triplet excitation energies, and oscillator strengths, using approximations of varying quality for both the xc potential and the xc kernel. This provides useful information on the appropriateness of the respective approximations for these systems.

In order to check whether or not the conclusions we draw from these atomic cases hold for molecules as well, we also consider some small molecules in the final part of the paper. Here we have to cope with the problem indicated above, that very accurate xc potentials do not exist for these systems. However, as will be explained later, we have constructed xc potentials which can be expected to improve upon existing approximate xc potentials for these systems, such as the LDA, generalized gradient approximated (GGA) and van Leeuwen–Baerends [35] (LB) potentials.

It can be expected that the improved potentials will yield improved results. However, the results with the usual potentials (especially the LB potential) are already quite satisfactory. It is therefore an open question whether much further improvement can be obtained by improving the xc potential, or that improvements to the xc kernel are more important. This is the question that will be addressed in the part of the paper dealing with the molecular case.

In the following section, the most important equations for the DFT linear-response calculations will be repeated and the relevant terms and equations will be introduced. After that, the technical details of the calculations will be given as well as the indications that our basis sets are very accurate. After this, our results will be discussed. First, the atomic polarizability results are treated. Then the excitation energies are discussed and compared to similar calculations which have very recently been performed by Petersilka *et al.* [18] and by Filippi *et al.* [32]. Finally, we present our molecular results and we end with some conclusions and suggestions for future work.

II. OUTLINE OF THE THEORY

DFT is based on the papers by Hohenberg and Kohn [33] and by Kohn and Sham [34]. The main result is that the density of a system is identical to the density of an associated noninteracting particle system, defined by the Kohn-Sham equations (atomic units are used throughout):

$$\left[-\frac{\nabla^2}{2}+v_s[\rho](\mathbf{r})\right]\phi_i(\mathbf{r})=\varepsilon_i\phi_i(\mathbf{r}). \tag{1}$$

Here $v_s[\rho](\mathbf{r})$ is the so-called Kohn-Sham potential, consisting of the external potential v_{ext} (the Coulomb field of the nuclei), the Hartree potential v_H, which is trivially calculated from the density, and the xc potential v_{xc}, which is the only unknown part:

$$v_s(\mathbf{r})=v_{ext}(\mathbf{r})+v_H(\mathbf{r})+v_{xc}(\mathbf{r}). \tag{2}$$

The xc potential v_{xc}, which is the functional derivative of the xc energy functional E_{xc} with respect to the density, has to be approximated in practical calculations. The most common approximations are the LDA and GGAs, although for response calculations the use of asymptotically correct xc potentials (such as the LB potential [35]) seems more appropriate. The xc potential determines the Kohn-Sham orbitals ϕ_i and their one-electron energies ε_i in Eq. (1). It also determines the density, which is obtained from the squares of the occupied Kohn-Sham orbitals times their occupation numbers f_i:

$$\rho(\mathbf{r})=\sum_i^{N_{occ}} f_i|\phi_i(\mathbf{r})|^2. \tag{3}$$

The exact xc potential, which is unique, yields the exact density of the system. This fact can be exploited to find a very accurate xc potential for systems for which a very accurate density is known. After having iteratively found the xc potential which generates the very accurate target density, one immediately obtains Kohn-Sham orbitals and one-electron energies to very good accuracy.

In the time-dependent extension of the Kohn-Sham equations, as proposed by Runge and Gross [9], a time-dependent Kohn-Sham potential $v_s(\mathbf{r},t)$ appears:

$$\left[-\frac{\nabla^2}{2}+v_s[\rho](\mathbf{r},t)\right]\phi_i(\mathbf{r},t)=i\frac{\partial}{\partial t}\phi_i(\mathbf{r},t). \tag{4}$$

The unknown xc part of this time-dependent Kohn-Sham potential is called the time-dependent xc potential $v_{\mathrm{xc}}(\mathbf{r},t)$. In linear-response calculations one needs the functional derivative $f_{\mathrm{xc}}(\mathbf{r},\mathbf{r}',t,t')$ of this time-dependent xc potential with respect to the time-dependent density $\rho(\mathbf{r},t)$:

$$f_{\mathrm{xc}}(\mathbf{r},\mathbf{r}',t,t')=\frac{\delta v_{\mathrm{xc}}(\mathbf{r},t)}{\delta\rho(\mathbf{r}',t')}, \tag{5}$$

which, as it depends on $t-t'$ only, can be Fourier transformed to $f_{\mathrm{xc}}(\mathbf{r},\mathbf{r}',\omega)$. This functional derivative f_{xc} is called the xc kernel and constitutes the second xc functional for which approximations have to be made in DFT response calculations. In nonlinear-response calculations, higher functional derivatives of $v_{\mathrm{xc}}(\mathbf{r},t)$ are needed as well [10,24,36], but usually these do not affect the results very much [37]. In this paper, we restrict ourselves to the linear-response case.

As f_{xc} is a function of two spatial variables and one frequency variable, it is rather complicated. However, the most usual and simplest approximation to it, the adiabatic LDA (ALDA), provides a very simple functional form for the xc kernel, by taking the derivative of the time-independent LDA expression for v_{xc} with respect to the density:

$$f_{\mathrm{xc}}^{\mathrm{ALDA}}(\mathbf{r},\mathbf{r}',\omega)=\delta(\mathbf{r}-\mathbf{r}')\frac{d^2}{d\rho^2}[\rho\varepsilon_{\mathrm{xc}}^{\mathrm{hom}}(\rho)]\big|_{\rho=\rho_0(\mathbf{r})}, \tag{6}$$

where $\varepsilon_{\mathrm{xc}}^{\mathrm{hom}}$ is the xc energy density of the homogeneous electron gas in the Vosko-Wilk-Nusair (VWN) approximation [38]. Evidently, this is a rough approximation to the exact f_{xc} as the frequency dependence is totally ignored (the adiabatic approximation assumes systems which are slowly varying in time), as is the spatial nonlocality of the kernel.

More refined approximations for the xc kernel are available. Petersilka and co-workers have introduced the time-dependent optimized effective potential (TDOEP) expression for the exchange part of the xc kernel [16,17]. In spin-unrestricted form, it is given by [16,18]

$$f_{\mathrm{x}\sigma\sigma'}^{\mathrm{TDOEP}}(\mathbf{r},\mathbf{r}',t,t')=-\delta(t-t')\,\delta_{\sigma\sigma'} \times\frac{\left|\sum_k f_{k\sigma}\phi_{k\sigma}(\mathbf{r})\,\phi_{k\sigma}^*(\mathbf{r}')\right|^2}{|\mathbf{r}-\mathbf{r}'|n_{0\sigma}(\mathbf{r})n_{0\sigma}(\mathbf{r}')}, \tag{7}$$

where $f_{k\sigma}$ is the occupation number of the KS spin orbital $\phi_{k\sigma}$ and where $n_{0\sigma}$ is the ground-state number density of the spin σ electrons. Although at present their expression still ignores the frequency dependence of f_{xc}, which is hard to model, their result should be very close to the exact exchange-only expression for the xc kernel in the limit $\omega\rightarrow 0$. A frequency-dependent extension of the ALDA expression has been provided by Gross and Kohn [39–42]. In this work, we will be using the ALDA expression for f_{xc} and its exchange-only counterpart.

In a linear-response calculation, we want to find the density change $\delta\rho(\mathbf{r},\omega)$, which is induced by a frequency-dependent external electric field $\delta v_{\mathrm{ext}}(\mathbf{r},\omega)$. In time-dependent density-functional linear-response theory, the density change does not depend on the external potential alone, but also on the potential which is induced by the density change through screening effects. The density change thus reacts to an *effective* potential δv_{eff} through the independent-particle linear-response equation:

$$\delta\rho(\mathbf{r},\omega)=\int d\mathbf{r}'\,\chi_s(\mathbf{r},\mathbf{r}',\omega)\,\delta v_{\mathrm{eff}}(\mathbf{r}',\omega). \tag{8}$$

Here, χ_s is the single-particle Kohn-Sham response function, constructed from occupied and virtual Kohn-Sham orbitals and one-electron energies [42,25]. This means that the exact xc potential will lead to the exact χ_s. The effective potential consists of the external potential δv_{ext} and two parts which depend upon the induced density $\delta\rho(\mathbf{r},\omega)$: the Coulomb or Hartree term and the xc term:

$$\delta v_{\mathrm{eff}}(\mathbf{r},\omega)=\delta v_{\mathrm{ext}}(\mathbf{r},\omega)+\int d\mathbf{r}'\,\frac{\delta\rho(\mathbf{r}',\omega)}{|\mathbf{r}-\mathbf{r}'|}+\delta v_{\mathrm{xc}}(\mathbf{r},\omega). \tag{9}$$

This implies that, if an exact xc potential is available, the only remaining unknown in Eq. (9) is the xc part to the screening, δv_{xc}. This xc part is given in terms of the Fourier transform of the xc kernel f_{xc} of Eq. (5):

$$\delta v_{\mathrm{xc}}(\mathbf{r},\omega)=\int d\mathbf{r}'\,f_{\mathrm{xc}}(\mathbf{r},\mathbf{r}',\omega)\,\delta\rho(\mathbf{r}',\omega). \tag{10}$$

An important advantage of the ALDA in practical applications, is that the evaluation of δv_{xc} in the integration points becomes a trivial multiplication of f_{xc} and $\delta\rho$, due to the delta function appearing in Eq. (6). For nonlocal kernels, such as the TDOEP kernel of Eq. (7), the evaluation of δv_{xc} in all integration points becomes an expensive computational task.

Equations (8)–(10) are solved self-consistently in an iterative fashion, starting from the uncoupled approximation ($\delta v_{\mathrm{eff}}=\delta v_{\mathrm{ext}}$) in Eq. (9). The induced density immediately yields the frequency-dependent polarizability tensor $\alpha_{ij}(\omega)$ [42,43,25] for a density change $\delta\rho_i(\mathbf{r},\omega)$ due to an external potential $\delta v_{\mathrm{ext}}(\mathbf{r},\omega)=\mathbf{r}_i\cos(\omega t)$:

$$\alpha_{ij}(\omega)=-2\int d\mathbf{r}\,\delta\rho_i(\mathbf{r},\omega)r_j, \tag{11}$$

where i and j denote the Cartesian directions x,y,z. We remark that in the actual implementation the polarizability is obtained as the trace of a matrix product of the first-order density matrix and the dipole moment matrix, which is equivalent to the integration in this equation.

By considering different multipole external electric fields, all multipole polarizabilities can be obtained. The excitation energies and oscillator strengths presented in this work [23] have been obtained along the lines of Refs. [19,13], using the same auxiliary basis functions techniques as in Ref. [25].

The singlet excitation energies and oscillator strengths obtained in this manner are directly related to the frequency-dependent polarizability $\alpha(\omega)$ by the relation

$$\alpha_{\mathrm{av}}(\omega)=\sum_i\frac{f_i}{\omega_i^2-\omega^2}, \tag{12}$$

where f_i are the oscillator strengths and ω_i the excitation energies, and where the average polarizability $\alpha_{\rm av}$ is equal to $(\alpha_{xx}+\alpha_{yy}+\alpha_{zz})/3$. The frequency dependence of this average polarizability is often expressed in terms of the Cauchy coefficients S_i:

$$\alpha_{\rm av}(\omega)=\sum_{k=1}^{\infty} S_{-2k}\omega^{2(k-1)}. \tag{13}$$

The Cauchy coefficients can be obtained from the excitation energies and oscillator strengths by the relation [13]

$$S_{-2k}=\sum_i \omega_i^{-2k} f_i . \tag{14}$$

In the basis-set limit, the Cauchy coefficient S_0 should be equal to the number of electrons. The coefficient S_{-2} is equal to the average static polarizability, as can be seen by substituting $\omega=0$ in Eq. (13).

In this work, we will approximate the screening part of $\delta v_{\rm eff}(\mathbf{r},\omega)$ in different ways. The approximation $\delta v_{\rm eff}=\delta v_{\rm ext}$ is called the uncoupled approximation, as screening is fully ignored. Taking into account Coulomb screening only, is equivalent to the approximation $f_{\rm xc}=0$. The results arising from this approximation will be denoted by ''Coulomb'' in the tables. The main part of the xc screening comes from the exchange part as could be expected. This will be shown by calculations in which we take $f_{\rm c}=0$, effectively using an $X\alpha$ form for $f_{\rm xc}$, with α equal to 2/3. This approximation will be denoted by ''Coulomb + f_x'' in the tables. The fully coupled results refer to the ALDA with the Vosko-Wilk-Nusair approximation to $\varepsilon_{\rm xc}$ [38]. They will be denoted by either ''ALDA'' or ''Coulomb + $f_{\rm xc}$.''

III. COMPUTATIONAL DETAILS

The Amsterdam density-functional program (ADF) [44–46] has been used for all calculations. The distinctive features of this program include the use of Slater-type orbitals (STOs), a well-balanced numerical integration scheme [45], a density fitting procedure for the Coulomb-type integrals using auxiliary basis functions (fit functions) [44], and a fully vectorized and parallelized code in combination with the use of symmetry [46]. The same features hold for the extension of ADF by which the response properties have been calculated [47].

A. Atomic calculations

In the atomic calculations on He, Be, and Ne, our goal has been to provide benchmark quality results with essentially exact xc potentials. For this reason we have tried to perform the calculations as accurately as possible. We included all electrons in the solution of the Kohn-Sham and the response equations. In other words, we did not use a frozen core approximation. The numerical integration accuracy was such that 12 significant digits were demanded for a representative set of test integrals (by default four significant digits are demanded). The convergence criterion in the self-consistent procedure for the solution of the Kohn-Sham equations was set to 10^{-12} (default value 10^{-6}).

We have tried to reach the basis-set limit by constructing large even-tempered STO basis sets. The final results and error margins have been obtained by comparing results from various basis sets of (very) high quality. The basis sets consist of several hundreds s, p, d, and f functions (higher angular momentum values are not available yet in ADF, but they are not needed in our present calculations) with both very diffuse and very contracted functions.

A typical basis set consists of 19 s functions, 20 p functions, 21 d functions, and 21 f functions, giving a total of 331 primitive basis functions. The most contracted functions of each type are a $1s$ function with exponent 20, a $2p$ function with exponent 20, a $3d$ function with exponent 40, and a $4f$ function with exponent 60. The most diffuse functions are $6s$, $6p$, $6d$, and $6f$ functions with exponents of 0.17 for one particular basis set. In other basis sets even more diffuse functions have been used, without significant change in the results.

The fit sets with s, p, d, f, and g functions have also been constructed in an even-tempered fashion, the most diffuse fit function being adapted to the most diffuse product of basis functions and the most contracted fit function adapted to the product of the most contracted basis functions. With these fit sets, which are clearly larger than the associated basis sets, typical fit errors (defined as the integral over all space of the squared difference between the exact and fitted converged SCF densities) of only 10^{-7} occurred. The most contracted fit functions possessed the smallest possible n value, while the most diffuse fit functions had an n value of 10 for all l values. The basis and fit sets are available for the interested reader [48].

For helium and beryllium the accuracy of our basis sets was confirmed by the fact that they reproduced the one-electron energies of Refs. [18] and [32,49] to all presented digits. For neon we have adopted the same basis sets. The accuracy of the basis sets is further supported by the values for the Cauchy moment S_0 of Eq. (13) which we obtained. In the basis-set limit, the value of S_0 (which is equal to the sum of the oscillator strengths) should equal the number of electrons. Typical deviations with our present basis sets are merely 10^{-3} to 10^{-6}, while for the largest basis sets in the ADF database, these errors are in the order of 0.1 to 1.

The accurate potentials were used in the following way. We used linear interpolation on the available accurate xc potential data, as provided by Umrigar and Gonze [30,31], in order to find the values of these potentials in the integration points generated by ADF. Afterwards, the Kohn-Sham equations were solved in these fixed xc potentials. As the number of points in which the accurate xc potentials were generated by Umrigar and Gonze is very large, the linear interpolation scheme will not influence our results by a significant amount. This is clear from the fact that we retrieve the KS orbital energies obtained by Savin *et al.* [49].

For the neon atom, there is no $v_{\rm xc}$ potential available of comparable accuracy. We have generated one from the STO CI density of Bunge and Esquivel [29]. This STO density is not sufficiently accurate in the outer region in order to allow for a straightforward determination of the xc potential in the whole $\mathbf{r}$ range. In the iterative procedure to determine the potential (the accurate updating procedure of Schipper *et al.* [27]), the potential was fixed in the outer region of the atom

for this reason, in order to obtain the correct asymptotic $-1/r$ behavior. The potential was constructed in such a way that it reached the $-1/r$ behavior at a certain cutoff point, beyond which the potential was taken identical to $-1/r$. The cutoff point was chosen in such a way that the orbital energy of the highest occupied KS orbital was very close to the experimental ionization energy (0.792 hartree). The resulting cutoff point was 6.72 a.u. Consequently, the accurate xc potential for Ne may be somewhat less accurate than the xc potentials for He and Be.

B. Molecular calculations

We have constructed molecular xc potentials which possess some important features which are typical of the exact xc potential and which recover our target Gaussian multireference configuration interaction (MRCI) density to reasonable accuracy. By construction, the potentials generated in our procedure will be smooth, possess the correct asymptotic $-1/r$ behavior, yield the experimental ionization potential for the highest occupied Kohn-Sham orbital, and are required to recover the MRCI density to reasonable accuracy. This final requirement ensures that the intershell peaks, exhibited by the exact xc potential, are present in our constructed potential as well.

The Hartree-Fock and subsequent direct (multireference) CI calculations, at the single-double excitation level, were performed with the ATMOL [50] package. The correlation energy which was recovered was 98% for H_2, 90% for HF, 82% for N_2, and typically around 75–80 % for the other molecules, when compared to the semiempirical correlation energy estimates of Savin *et al.* [51].

Correlation-consistent GTO basis sets of at least valence triple zeta quality were used, to which sets of diffuse functions were added. The basis set sizes were different depending on the molecule. Our aim was to take a reliable correlation-consistent basis set including diffuse functions. Typically, we took Woon and Dunning's [52] doubly or in most cases triply augmented correlation-consistent (cc) valence triple zeta (VTZ) basis sets denoted by d-aug-cc-pVTZ or t-aug-cc-pVTZ. We have also performed calculations with correlation-consistent quadruple zeta basis sets to which we added some diffuse functions ourselves. The total number of GTOs was typically between 100 and 150.

We have further used the straightforward scheme of Ref. [35] for updating the xc potential until the density resulting from the KS calculation with that xc potential was sufficiently close to the target CI density. We used an asymptotically correct initial guess for the xc potential of the form

$$v_{\mathrm{xc}}(\mathbf{r}) = v_{X\alpha}(\mathbf{r}) + 2\varepsilon_c^{\mathrm{VWN}}(\mathbf{r}) + 2\varepsilon_x^{\mathrm{Becke}}(\mathbf{r}), \qquad (15)$$

consisting of the $X\alpha$ potential, the Vosko-Wilk-Nusair parametrization of the LDA correlation energy density, and the Becke energy functional for the correction to the $X\alpha$ exchange. This last term ensures the correct asymptotic $-1/r$ behavior. This initial guess has been successfully employed several times before [53].

Because of the known problems [27] which arise, in case of a Gaussian CI density, if the potential is converged completely (such as spurious oscillations and incorrect asymptotic behavior), the updating scheme was changed in such a fashion that the outer region of the potential was left virtually unchanged [53], so as to retain its asymptotically correct behavior. The updating scheme slowly converges to the (undesirable) exact xc potential. After a hundred cycles, the integrated absolute density error with respect to the CI density, as defined in Ref. [27], has typically dropped to a satisfactory 10^{-2} or 10^{-3}. Further convergence hardly improves this difference, but it does introduce the spurious oscillations mentioned before. For this reason we used, as recommended [27], the potentials which appeared after a hundred cycles. The parameter α of the starting $X\alpha$ potential was chosen such that the eigenvalue of the highest occupied Kohn-Sham orbital $\varepsilon^{\mathrm{HOMO}}$, belonging to the final potential, equals minus the ionization potential, as it should.

The potentials, which have all been constructed in this manner, can certainly not be called exact, and our method of construction severely restricts the freedom of the potential. For example, the distance at which the potential gets close to the $-1/r$ behavior is predominantly determined by the start-up potential. However, our results did not change very much if another start-up potential with correct asymptotic behavior was used. On the other hand, if the α parameter in the start-up potential was not adapted in order to obtain the experimental ionization potential, relatively poor results were obtained.

Although the potentials will not be the exact ones, which belong to the exact (not the GTO-CI) correlated densities, there are good reasons to assume that the constructed potentials improve upon the xc potentials which were used in previous DFT response calculations, such as the usual potentials belonging to the LDA or GGAs or the asymptotically correct Van Leeuwen–Baerends potential [35] (LB). These potentials all exhibit one or several distinct weaknesses, such as the faster than Coulombic decay of the potential in the outer region (LDA and GGAs), inferior values for the highest occupied Kohn-Sham orbital which should equal minus the experimental ionization energy (LDA and GGAs), poor description or absence of the intershell peaks (LDA, GGAs, and LB), and poor description of the inner region of the atoms in the molecule (LB).

IV. RESULTS AND DISCUSSION

A. Atomic results, polarizabilities

In Table I, the dipole and quadrupole polarizabilities are presented for the three atoms which are studied here. The results for He and Ne with the LDA and LB potentials are somewhat more accurate than our previous results [25,12] due to the removal of the frozen core approximation for Ne and the improvements in the basis sets. As expected, this has led to slightly higher values for the polarizabilities. The LDA dipole polarizabilities of He and Ne are now in perfect agreement with the numerical results reported in Table 4.4 of Ref. [43], showing that our results are very close to the basis set limit. The quadrupole polarizability results are not identical to those obtained by Mahan [54], because the Gunnarsson-Lundqvist parametrization [55] for v_{xc} was used in that work.

It has been emphasized several times [56,12] that the usual xc potentials, such as the LDA potential, overestimate the polarizabilities due to their incorrect asymptotic behav-

TABLE I. Dipole and quadrupole polarizabilities of helium, beryllium, and neon with various xc potentials using the ALDA for f_{xc}.

Polarizability	Atom	LDA[a]	LB[b]	Accurate v_{xc}[c]	Literature
Dipole	He	1.6576	1.3896	1.3824	1.3832[d]
	Be	43.79 ± 0.02	42.87 ± 0.01	39.57 ± 0.01	37.73 ± 0.05[e]
	Ne	3.049 ± 0.003	2.590	(2.657)	2.670[f]
Quadrupole	He	3.576	2.561	2.538	2.4451[d]
	Be	369.9 ± 0.5	342.4 ± 0.5	300.4 ± 0.5	298.8[g]; 298.8 ± 2.6[h]
	Ne	9.66 ± 0.02	7.26 ± 0.03	(7.52 ± 0.02)	7.52[i]; (7.33[j])

[a]The VWN [38] parametrization is used.

[b]The Van Leeuwen–Baerends model potential [35].

[c]Accurate xc potential due to Umrigar and Gonze [30]; for Ne, the potential constructed from the Bunge-Esquivel STO CI density was used (see text).

[d]Benchmark *ab initio* calculation using explicitly correlated wave functions [57].

[e]Recent basis-set limit result obtained with the explicitly correlated coupled-cluster method [68].

[f]Value obtained by comparison of many experimental data [58].

[g]Coupled-cluster double-excitation value with fourth-order contribution from singlet and triplet excitations [69].

[h]Fourth-order Møller-Plesset perturbation theory value [70].

[i]Coupled-cluster singles-doubles value, with an approximate triples contribution [CCSD(T)] [71].

[j]Second-order many-body perturbation theory value [72].

ior. This is obvious in Table I. The LDA dipole polarizabilities are too high by 19.8%, 16.1%, and 14.2% respectively, while the LDA quadrupole polarizabilities are too high by 46.3%, 23.8%, and 28.3%. The asymptotically correct LB potential already improves considerably upon this. The errors for this potential are +0.46%, +13.6%, and −3.0% for the dipole polarizabilities. For the quadrupole polarizabilities, the numbers are +4.7%, +14.6%, and −3.2%. The accurate xc potential improves upon the LDA and LB results in all six cases. For the dipole polarizabilities, the errors are −0.06%, +4.9%, and −0.5%, while the quadrupole polarizability errors are +3.80%, +0.54%, and 0.0%, respectively.

In order to investigate how sensitive these properties are with respect to small changes in the xc potential, we have repeated the Be calculations not with the Umrigar-Gonze potential, but with another accurate xc potential, constructed from the Esquivel-Bunge CI STO density [28], in the same way as we construct our Ne potential from an STO CI density by Bunge and Esquivel [29].

The xc potential for Be by Umrigar and Gonze [30] should be considered more reliable than the present one, but these test calculations give an indication of how much our neon results may still differ from results with the truly exact xc potential. We find a dipole polarizability of 40.01 ± 0.01 (instead of 39.57 with the Umrigar-Gonze potential) and a quadrupole polarizability of 309.2 ± 0.2 (instead of 300.4) with the xc potential constructed from the Esquivel-Bunge density for Be. The differences with respect to the results with the accurate potential by Umrigar and Gonze are considerable. For this reason we have given the Ne results in parentheses in Table I, although we expect the results with the Bunge-Esquivel density for the rare gas Ne to be more reliable than those for Be.

The average absolute error for all six numbers in Table I is reduced by roughly a factor of 4 by going from the LDA potential to the LB potential. The average absolute error with the accurate xc potential is again a factor of 4 smaller than the average absolute LB error, and a factor of 15 smaller than the LDA error. For these atomic polarizabilities it is consequently clear that improvements to the xc potential will yield the bulk of the improvement which can be obtained. The remaining errors have to be due to deficiencies in the xc kernel f_{xc}. As we are considering static polarizabilities, these deficiencies relate to the spatial variables, not to the frequency dependence.

In four cases out of six, the accurate xc potential results for the polarizabilities of these atoms can be called excellent. The errors for the quadrupole polarizability of He(+3.8%) and the dipole polarizability of Be(+4.9%) are, however, still substantial. Upon closer analysis, the dipole polarizability of Be appears to depend strongly on the description of the $2s \rightarrow 2p$ transition (the reason for the different dipole polarizability obtained with the Esquivel-Bunge density is also that this transition is differently described). For this analysis, it is useful to look at Eq. (12), which expresses the polarizability in terms of the oscillator strengths f_i and the excitation energies ω_i. Using this equation for the present static case ($\omega = 0$), we find that about 95% of the polarizability of Be is due to the (singlet) $2s \rightarrow 2p$ transition. For this transition, we obtained an oscillator strength of 1.339 a.u. (having taken the degeneracy of the p orbitals into account) and an excitation energy of 0.1868 hartree, as will be shown in one of the following tables. The experimental value for the excitation energy is 0.1939 hartree. Our excitation energy with the accurate xc potential is consequently too low by 3.7%. This should lead to an overestimation in the contribution of the $2s \rightarrow 2p$ transition to the polarizability of no less than 7.7%. Apparently, the oscillator strength for this transition is underestimated, leading to a fortuitous cancellation of errors. In short, the error in the predicted dipole polarizability of beryllium, obtained with the accurate xc potential, can be

TABLE II. Dipole and quadrupole polarizabilities of helium, beryllium, and neon with various xc kernels using the accurate xc potential.

Polarizability	Atom	Uncoupled	Coulomb	Coulomb+f_x	Coulomb+f_{xc}	Literature
Dipole	He	1.5158	1.2231	1.3665	1.3824	1.3832 [57]
	Be	73.98	29.36	37.99	39.57	37.73±0.05 [68]
	Ne	3.063	2.417	2.632	2.657	2.67 [58]
Quadrupole	He	2.452	2.385	2.518	2.538	2.4451 [57]
	Be	283.7	251.8	291.5	300.4	298.8±2.6 [70]
	Ne	7.39	6.98	7.45	7.52	7.52 [71]

fully explained from the inability of the ALDA xc kernel to describe the $2s\rightarrow 2p$ transition with sufficient accuracy. In passing, we note that the $2s\rightarrow 2p$ transition in Be is the only atomic transition we consider, which is close in energy to excitation energies normally encountered in molecules.

In Table II, the importance of the various contributions to the screening is tabulated. As explained in the introductory section, the ''uncoupled'' results refer to a total neglect of screening, which is equivalent to the approximation $\delta v_{\mathrm{eff}} = \delta v_{\mathrm{ext}}$ in Eq. (9). The uncoupled results for the dipole polarizability are far too large in all three cases (this is also the usual case in molecular dipole polarizability calculations), while the uncoupled quadrupole polarizabilities are much closer to the experimental values. Interestingly, the uncoupled quadrupole polarizabilities are too low for Be and Ne and slightly too high for He.

In agreement with Ref. [13], we find that the inclusion of the Coulomb screening in the second column (this is the approximation $f_{\mathrm{xc}}=0$) substantially reduces all the uncoupled polarizabilities and leads to too low values with respect to experiment in all six cases. In the column denoted by ''Coulomb + f_x,'' the exchange part of the screening is included, using the Vosko-Wilk-Nusair (VWN) exchange functional (which is equivalent to the $X\alpha$ parametrization with $\alpha=2/3$). It is clear from the table that the exchange part constitutes the major part of the xc screening, as could be expected.

Finally, in the last two columns we have copied the fully coupled (both exchange and correlation screening included in the xc kernel) and experimental or *ab initio* values from Table I, for ease of comparison. The inclusion of the correlation part of the screening substantially reduces the errors in four cases out of six. In the other two cases (those with the largest deviations with respect to the benchmark values) the results get somewhat worse.

In the rest of this work, it will be shown that the fully coupled calculations for the excitation energies of helium hardly differ from the uncoupled values (the differences between occupied and virtual KS orbital energies), which are already excellent. In view of this fact, it may be somewhat surprising that the fully coupled (both Coulomb and xc screening taken into account) result for the static dipole polarizability of helium is considerably better than the uncoupled value. This must of course be due to the improved results for the oscillator strengths which appear in Eq. (12).

In Table III, these fully coupled oscillator strengths for He, calculated with the accurate xc potential, are compared to the literature values. Here, it becomes clear that the excellent result for the static dipole polarizability of helium does not hold for the individual oscillator strengths. The contribution of the $1s\rightarrow 2p$ transition to the dipole polarizability, using our ALDA values for the oscillator strength and the excitation energy in Eq. (12), is 0.471 a.u. The literature values for the excitation energy and the oscillator strength yield a contribution of only 0.454 a.u. This is counterbalanced by the other oscillator strengths, which are a bit too low. We note, however, that only the exact frequency dependent xc kernel can be expected to give the individual oscillator strengths and excitation energies correctly.

Because the static dipole polarizability of He comes out so nicely with the accurate xc potential, it is interesting to see if this remains so in the frequency dependent case. In the static polarizability calculations, the spatial part of the xc kernel is tested. In a frequency-dependent run, one also tests the frequency-dependence of this kernel. In other words, one tests how well the adiabatic approximation holds when the frequency of the external field approaches the first excitation energy with nonvanishing oscillator strength.

Our results for the frequency dependence of the dipole polarizability of He are gathered in Table IV, as well as in Fig. 1. The LDA results are far too large and increase too sharply with increasing frequency. This is of course related to the position of the first pole, which appears much too early with the LDA potential. The LB results are already much better, but the results with the accurate xc potential are closest to the benchmark results (taken from highly accurate *ab initio* calculations with explicitly correlated wave functions [57]). This holds both for the results with the full ALDA and with the exchange-only ($X\alpha$) approximation for f_{xc}. However, the figure shows that it is not possible to ignore the xc screening altogether, as the accurate v_{xc}-Coulomb curve is quite poor. This was to be expected in view of the poor corresponding static result in Table II. So it appears that both an accurate v_{xc} and a reasonable approximation for f_{xc} are

TABLE III. Helium oscillator strengths.

Transition	Exact[a]	ALDA[b]
$1s\rightarrow 2p$	0.27616	0.283 (+2.5%)
$1s\rightarrow 3p$	0.07343	0.0698 (−4.9%)
$1s\rightarrow 4p$	0.02986	0.0282 (−5.5%)
$1s\rightarrow 5p$	0.01504	0.0142 (−5.5%)
$1s\rightarrow 6p$	0.00863	0.0082 (−5.0%)

[a]Accurate nonrelativistic theoretical calculations [73,74].
[b]Results with accurate xc potential and ALDA for f_{xc}.

TABLE IV. Frequency dependence of the dipole polarizability of helium with various xc potentials.

Frequency (hartree)	Exact[a]	Acc.-ALDA[b]	Acc.–x-only[c]	Acc.-Coulomb[d]	LDA[e]	LB[f]
0	1.383	1.382	1.366	1.223	1.658	1.390
0.1	1.399	1.398	1.382	1.236	1.682	1.406
0.2	1.448	1.448	1.431	1.276	1.763	1.456
0.3	1.541	1.542	1.522	1.350	1.921	1.551
0.4	1.698	1.701	1.677	1.475	2.219	1.713
0.5	1.970	1.979	1.946	1.686	2.883	1.996
0.6	2.508	2.537	2.480	2.090	pole[g]	2.571
0.7	4.116	4.286	4.114	3.192	pole	4.490

[a]Benchmark *ab initio* calculation using explicitly correlated wave functions [57].
[b]Results with accurate xc potential due to Umrigar and Gonze [30] with ALDA approximation for f_{xc}.
[c]Results with accurate xc potential due to Umrigar and Gonze [30] with exchange-only ($X\alpha$) approximation for f_{xc}.
[d]Results with accurate xc potential due to Umrigar and Gonze [30] with approximation $f_{xc}=0$.
[e]The VWN parametrization is used [38].
[f]Van Leeuwen–Baerends potential [35].
[g]For LDA, the first pole appears before 0.6 hartree.

needed for reliable results here.

For the accurate v_{xc}-ALDA results, the deviation in the frequency range of 0 to 0.3 hartree is less than 0.1% from the literature values. For higher frequencies, the deviations are not negligible anymore. At 0.7 hartree, in the neighborhood of the pole, the accurate v_{xc}-ALDA result overshoots by 4%. Interestingly, in this region the accurate v_{xc}–exchange-only f_{xc} are the best, in contrast to the situation at zero frequency.

One might be tempted to blame this solely on the adiabatic approximation (the neglect of frequency dependence in the xc kernel), which is supposed to break down in the vicinity of a pole. This breakdown is due to the fact that the position of this pole, which determines the polarizability in the frequency region near that pole, is only given correctly by the exact frequency-dependent xc kernel. The exact static xc kernel will give a different position of the first pole, with large effects for the frequency-dependent polarizability near the pole, as is clear from Eq. (12). However, this question cannot be answered unless one would know the polarizability result with the (unknown) exact static f_{xc}. This result should be equal to the experimental number at $\omega=0$, but will differ from the ALDA result at finite frequencies, in case this static result is obtained from different values for the oscillator strengths and excitation energies (especially those belonging to the first pole). If one recalculates the polarizability with the experimental values for the excitation energy and oscillator strength of the $1s\rightarrow 2p$ transition, the result is even somewhat below the exact literature value at $\omega=0.7$ hartree (4.07 a.u.). The overestimated value for the oscillator strength and the underestimated value for the first excitation energy are responsible for the overestimated polarizability at larger frequencies in roughly equal amounts.

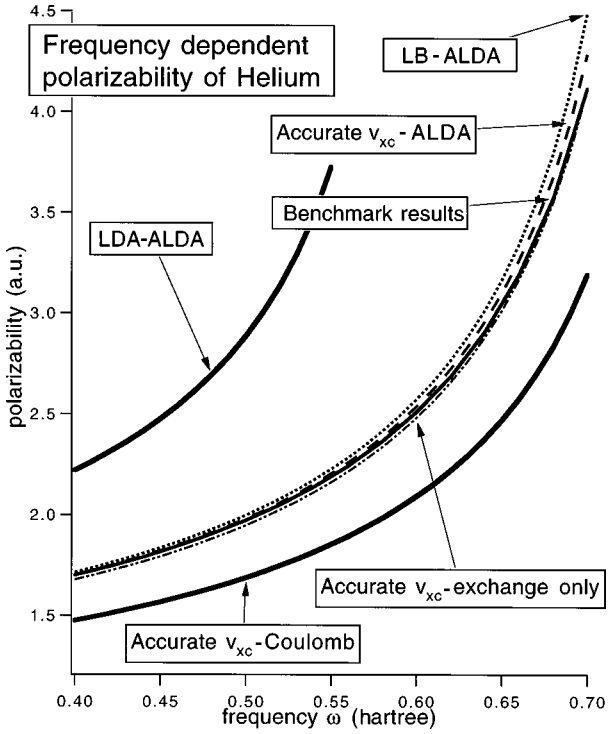

FIG. 1. The dynamic polarizability of He calculated with different xc potentials and xc kernels.

We have checked whether the curve with the accurate xc potential improves if one employs Gross and Kohn's frequency-dependent xc kernel [39–42], instead of the ALDA f_{xc}. This is not the case. The Gross-Kohn (GK) kernel indeed lowers the frequency dependence, but the correction is far too large, resulting in a curve which is too low in the whole frequency range (1.49 a.u. at 0.3 hartree and 2.31 a.u. at 0.6 hartree). Furthermore, an unphysical anomalous frequency dispersion appears in the very low frequency region. This behavior can be understood from the frequency dependence of the real part of the GK kernel. If the frequency becomes larger than zero, the absolute value of the real part of the GK kernel decreases. The xc screening is reduced in this way. The magnifying effect of this screening (see the results of Table II) on the polarizability also reduces, leading to a polarizability which *decreases* with increasing frequency (for very small frequencies).

For the Cauchy coefficient S_{-4}, which describes the frequency dependence of the dipole polarizability in the low

frequency region, we obtain 1.554 ± 0.001 with the accurate xc potential. A fit to the literature data [57] yields a value of 1.54 ± 0.01. Apparently the fit to the experimental data [58], resulting in a value of 1.60, in Ref. [59] overestimates the frequency dependence of the dipole polarizability in the low frequency region somewhat.

The LDA and LB results for this coefficient are 2.432 ± 0.001 and 1.573 ± 0.001, respectively. For the coefficient S_{-6} we obtain LDA and LB results of 4.462 ± 0.002 and 2.127 ± 0.002, respectively. The accurate potential yields 2.086 for S_{-6}. For the higher Cauchy coefficients, the importance of the first transition with nonvanishing oscillator strength increases, as can be seen from Eq. (14). In view of the overestimated oscillator strength and underestimated excitation energy for this transition with the accurate xc potential, the S_{-4} and S_{-6} can be expected to be somewhat too large.

For the Cauchy coefficients of Be, we find 1.35×10^3, 1.36×10^3, and 1.105×10^3 for S_{-4} using the LDA, LB, and accurate xc potentials, respectively. The numbers for the S_{-6} coefficient are 4.26×10^4, 4.43×10^4, and 3.155×10^4. These results, even those from the accurate potential, are too large because of the inaccurate description of the $2s \rightarrow 2p$ transition. A correction on these values, based upon the coupled cluster value of the static polarizability of 37.73, and the experimental excitation energy, would yield (semiempirical) estimates of $(1.0 \pm 0.1) \times 10^3$ and $(2.6 \pm 0.2) \times 10^4$ for S_{-4} and S_{-6}, respectively.

B. Atomic results, excitation energies of helium

In this section we discuss our results for the excitation energies. Recently, Savin, Umrigar, and Gonze have shown [49] that the exact Kohn-Sham one-electron energy differences between the highest occupied Kohn-Sham orbital and virtual orbitals provide quite satisfactory approximations to excitation energies for helium and beryllium. The orbital energy differences lie between the experimental singlet and triplet excitation energies, almost without exception.

Going beyond this, Filippi, Umrigar, and Gonze [32] calculated excitation energies using two perturbative schemes. One of these first-order perturbative schemes, based upon Görling and Levy's adiabatic connection approach [60,61], improves upon the orbital energy difference approximation to the excitation energies. We have included these results in the tables. The other results obtained by Filippi *et al.* are based on ordinary perturbation theory and provide no improvement over the Kohn-Sham orbital energy differences. These results will not be discussed here.

Petersilka, Gossmann, and Gross [18] have recently calculated excitation energies for helium with Umrigar and Gonze's accurate xc potential [30], using the TDDFT approach. They present numerical results using the ALDA and TDOEP xc kernels, both in their single-pole approximation (SPA) and by diagonalizing a matrix containing contributions from as many bound Kohn-Sham orbitals as were needed for converged results. For ease of reference we repeat their equations [18] for the SPA excitation energies here, for an excitation from occupied orbital ϕ_i to virtual orbital ϕ_a:

$$\omega_{\mathrm{sing}} = (\varepsilon_a - \varepsilon_i) + 2\ \mathrm{Re} \int d^3\mathbf{r} \int d^3\mathbf{r}'\, \phi_i^*(\mathbf{r})\, \phi_a^*(\mathbf{r}) \times \left(\frac{1}{|\mathbf{r}-\mathbf{r}'|} + \frac{1}{4}[f_{\mathrm{xc}}^{\uparrow\uparrow} + f_{\mathrm{xc}}^{\uparrow\downarrow} + f_{\mathrm{xc}}^{\downarrow\uparrow} + f_{\mathrm{xc}}^{\downarrow\downarrow}] \right) \phi_i(\mathbf{r}')\, \phi_a(\mathbf{r}'),$$

$$\omega_{\mathrm{trip}} = (\varepsilon_a - \varepsilon_i) + 2\ \mathrm{Re} \int d^3\mathbf{r} \int d^3\mathbf{r}'\, \phi_i^*(\mathbf{r})\, \phi_a^*(\mathbf{r}) \times \left(\frac{1}{4}[f_{\mathrm{xc}}^{\uparrow\uparrow} - f_{\mathrm{xc}}^{\uparrow\downarrow} - f_{\mathrm{xc}}^{\downarrow\uparrow} + f_{\mathrm{xc}}^{\downarrow\downarrow}] \right) \phi_i(\mathbf{r}')\, \phi_a(\mathbf{r}'), \quad (16)$$

where ε_i and ε_a are KS orbital energies and where $f_{\mathrm{xc}}^{\sigma\sigma'}$ is a shorthand notation for $f_{\mathrm{xc}}^{\sigma\sigma'}(\mathbf{r},\mathbf{r}',\omega_0)$, which is the Fourier transform of the functional derivative

$$f_{\mathrm{xc}}^{\sigma\sigma'}(\mathbf{r},t,\mathbf{r}',t') = \frac{\delta v_{\mathrm{xc}}^{\sigma}(\mathbf{r},t)}{\delta \rho^{\sigma'}(\mathbf{r}',t')}. \quad (17)$$

Combining these expressions yields the SPA expression for the singlet-triplet splitting

$$\omega_{\mathrm{sing}} - \omega_{\mathrm{trip}} = \mathrm{Re} \int d^3\mathbf{r} \int d^3\mathbf{r}'\, \phi_i^*(\mathbf{r})\, \phi_a^*(\mathbf{r}) \times \left(\frac{2}{|\mathbf{r}-\mathbf{r}'|} + f_{\mathrm{xc}}^{\uparrow\downarrow}(\mathbf{r},\mathbf{r}',\omega_0) + f_{\mathrm{xc}}^{\downarrow\uparrow}(\mathbf{r},\mathbf{r}',\omega_0) \right) \times \phi_i(\mathbf{r}')\, \phi_a(\mathbf{r}'), \quad (18)$$

where $f_{\mathrm{xc}}^{\uparrow\downarrow}$ is equal to $f_{\mathrm{xc}}^{\downarrow\uparrow}$ for closed-shell systems, as are $f_{\mathrm{xc}}^{\uparrow\uparrow}$ and $f_{\mathrm{xc}}^{\downarrow\downarrow}$.

Their approach should yield the same results as ours, provided that our basis set is sufficiently large. We have checked that the orbital energy differences are identical to those obtained by Petersilka *et al.* [18] for He, and those by Savin *et al.* [49] for He and Be. We have furthermore checked that we could reproduce the ALDA-SPA results by Petersilka *et al.*, by calculating the required matrix elements. The SPA results were identical, except for a single deviation of only 0.1 mhartree. We have also confirmed that the implementations of f_{xc} and G_{xc} are identical [62].

However, it appeared that our fully coupled ALDA results were not identical to those obtained by Petersilka *et al.* by diagonalizing a large matrix. The reason for this, as suggested by Petersilka [62], is that in their numerical program, continuum contributions cannot be taken into account, while our basis set program provides a (discrete) description of the continuum through the virtual orbitals with positive one-electron energies. This was verified by only taking into account virtuals with negative one-electron energies in our calculations. In this way we recovered the results obtained by Petersilka *et al.* It will be shown below that this continuum contribution considerably improves some of the results.

TABLE V. Helium singlet excitation energies (in hartrees).

Transition	Exact[a]	KS eigenvalues[b]	ALDA,bound[c]	TDOEP-SPA or PT[d]	ALDA, full [e]
$1s\rightarrow 2s$	0.7578	0.7460	0.7678	0.7687	0.7608
$1s\rightarrow 3s$	0.8425	0.8392	0.8461	0.8448	0.8435
$1s\rightarrow 4s$	0.8701	0.8688	0.8719	0.8710	0.8706
$1s\rightarrow 5s$	0.8825	0.8819	0.8835	0.8830	0.8828
$1s\rightarrow 6s$	0.8892	0.8888	0.8898	0.8894	0.8893
$1s\rightarrow 2p$	0.7799	0.7772	0.7764	0.7850	0.7751
$1s\rightarrow 3p$	0.8486	0.8476	0.8483	0.8500	0.8479
$1s\rightarrow 4p$	0.8727	0.8722	0.8726	0.8732	0.8724
$1s\rightarrow 5p$	0.8838	0.8836	0.8838	0.8841	0.8837
$1s\rightarrow 6p$	0.8899	0.8898	0.8899	0.8901	0.8898
Av. abs. error (mhartrees)[f]		2.2	2.1	2.2	1.0

[a]Accurate nonrelativistic calculations by Drake [73].
[b]Zeroth-order approximation provided by differences in KS eigenvalues.
[c]ALDA results obtained by taking into account all bound KS orbitals [18].
[d]Values obtained with TDOEP kernel in the SPA [18] or by DFT perturbation theory [32]. The results for the higher transitions are given in Ref. [18] only.
[e]This work, ALDA results obtained by taking into account all bound and unbound KS orbitals.
[f]The average absolute error with respect to the ''exact'' values is given in mhartrees.

In Table V, several results for the singlet excitation energies of helium have been gathered. It is clear that the orbital energy differences in the third column already provide good approximations to the experimental excitation energies. The average absolute deviation is only 2.2 mhartree from the experimental values. Petersilka's fully coupled ALDA results with bound orbitals yield a similar deviation of 2.1 mhartree.

The best results by Filippi *et al.* [32] have been given in the fourth column. These results are in fact identical to the SPA results obtained by Petersilka *et al.* with the TDOEP approximation for f_{xc}. This can be understood from the fact that, for two-electron systems, both approaches reduce to the calculation of the same Coulomb-type matrix element [compare the appendix of Ref. [32] and Eq. (7)]. Both approaches give a first-order exchange-only correction to the orbital energy differences. The results obtained by Filippi *et al.* give no improvement over the ALDA results obtained by Petersilka *et al.*

Our fully coupled ALDA results, which have converged with respect to basis set size, are given in the last column. The deviation with respect to the experimental values drops by a factor of 2 in comparison to the results obtained by Petersilka *et al.* and those obtained by Filippi *et al.* The average absolute deviation is 1.0 mhartree for our results. We emphasize that the only difference between our results in the final column and those obtained by Petersilka *et al.* is the inclusion of virtual orbitals with positive one-electron energies in our calculation [62]. It is the contribution of the continuum that ensures the improvement in the results. One can speculate that a similar improvement could be obtained for the TDOEP kernel, if a fully coupled calculation would be performed. It is too early to conclude that the ALDA performs better than the TDOEP for these transitions.

It is interesting to note that the last three columns of Table V all correct the $s\rightarrow s$ orbital energy differences in the right direction with respect to the experimental values, but by too large amounts. For the $s\rightarrow p$ transitions, the ALDA corrections to the orbital energy differences are again in the right direction, but for these transitions the correction is not large enough. The notable exception is the $2s\rightarrow 2p$ transition. Here, the ALDA correction actually makes the result worse. The first-order exchange-only results of Filippi *et al.* are worse than the ALDA results for the singlet $s\rightarrow s$ and $s\rightarrow p$ transitions.

In Table VI, the triplet excitation energies corresponding to the singlet excitation energies of Table V are presented. Here, all results clearly improve upon the orbital energy differences. Contrary to what was seen in the previous table, the two sets of ALDA results do not differ much in accuracy here. The inclusion of the continuum contribution plays less of a role than in the singlet case and also Filippi *et al.*'s exchange-only results are hardly worse than the fully coupled ALDA results. The exchange-only results again overcorrect the orbital energy differences, as in the singlet case, for the $s\rightarrow s$ transitions. The ALDA results give too small corrections for these transitions. All coupled results for the $s\rightarrow p$ transitions are quite satisfactory.

Now we turn to the singlet-triplet splittings for these transitions in Table VII. Here, the ALDA results are clearly better than the exchange-only results. The exchange-only results give too high splittings, as already observed by Petersilka *et al.* [17,18]. This is due to the fact that the corrections to the orbital energy differences are too large in the exchange-only case, for both the singlet and the triplet energies.

In the ALDA results a cancellation of errors occurs, as the singlet and triplet excitation energies are both too high for the $s\rightarrow s$ transitions. For this reason, the ALDA singlet-triplet splittings come out more accurately than the excitation energies themselves. From this table, it is obvious that the continuum contribution is of importance and helps to further improve upon Petersilka's ALDA results. The final average

TABLE VI. Helium triplet excitation energies (in hartrees).

Transition	Exact[a]	KS eigenvalues[b]	ALDA,bound[c]	TDOEP-SPA or PT [d]	ALDA,full[e]
$1s\rightarrow 2s$	0.7285	0.7460	0.7351	0.7232	0.7334
$1s\rightarrow 3s$	0.8350	0.8392	0.8368	0.8337	0.8362
$1s\rightarrow 4s$	0.8672	0.8688	0.8679	0.8667	0.8677
$1s\rightarrow 5s$	0.8811	0.8819	0.8815	0.8808	0.8813
$1s\rightarrow 6s$	0.8883	0.8888	0.8885	0.8882	0.8885
$1s\rightarrow 2p$	0.7706	0.7772	0.7698	0.7693	0.7689
$1s\rightarrow 3p$	0.8456	0.8476	0.8457	0.8453	0.8454
$1s\rightarrow 4p$	0.8714	0.8722	0.8715	0.8712	0.8713
$1s\rightarrow 5p$	0.8832	0.8836	0.8832	0.8831	0.8831
$1s\rightarrow 6p$	0.8895	0.8898	0.8895	0.8895	0.8895
Av. abs. error (mhartrees)[f]		3.5	1.1	0.9	0.9

[a]Accurate nonrelativistic calculations by Drake [73].
[b]Zeroth-order approximation provided by differences in KS eigenvalues.
[c]ALDA results obtained by taking into account all bound KS orbitals [18].
[d]Values obtained with TDOEP kernel in the SPA [18] or by DFT perturbation theory [32]. The results for the higher transitions are given in Ref. [18] only.
[e]This work, ALDA results obtained by taking into account all bound and unbound KS orbitals.
[f]The average absolute error with respect to the ''exact'' values is given in mhartrees.

absolute error for the fully coupled ALDA results in the last column is a very satisfactory 0.6 mhartree, which clearly improves upon both the ALDA results with bound KS orbitals only and the exchange-only values based on DFT perturbation theory (PT).

C. Atomic results, excitation energies of beryllium

Now we turn to the excitation energies of beryllium. The singlet excitation energies are given in Table VIII. For the LDA potential, only the first couple of excitation energies have been given. Those are the only transitions to virtuals which are bound in the LDA potential. Not surprisingly, no reliable values for higher excitation energies could be obtained. The ordering of the excitations even differs from the experimental ordering. We can conclude that the LDA potential does not give a qualitatively correct description of all but the lowest excitations in Be.

For the LB potential, results for the lowest four excitation energies are given. For higher excitations, relatively large differences between results in different basis sets occurred. This is due to the long range of the LB potential, which leads

TABLE VII. Helium singlet-triplet splittings (in millihartrees).

Transition	Exact[a]	ALDA,bound[b]	TDOEP-SPA or PT[c]	ALDA,full[d]
$1s\rightarrow 2s$	29.3	32.7	45.5	27.4
$1s\rightarrow 3s$	7.4	9.4	11.1	7.3
$1s\rightarrow 4s$	2.9	4.0	4.3	2.9
$1s\rightarrow 5s$	1.4	2.1	2.2	1.4
$1s\rightarrow 6s$	0.8	1.3	1.2	0.8
$1s\rightarrow 2p$	9.3	6.6	15.7	6.2
$1s\rightarrow 3p$	2.9	2.6	4.7	2.5
$1s\rightarrow 4p$	1.3	1.1	2.0	1.1
$1s\rightarrow 5p$	0.6	0.6	1.0	0.6
$1s\rightarrow 6p$	0.4	0.3	0.6	0.3
Av. abs. error (mhartrees)[e]		1.1	3.2	0.6

[a]Accurate nonrelativistic calculations by Drake [73].
[b]ALDA results obtained by taking into account all bound KS orbitals [18].
[c]Values obtained with TDOEP kernel in the SPA [18] or by DFT perturbation theory [32]. The results for the higher transitions are given in Ref. [18] only.
[d]This work, ALDA results obtained by taking into account all bound and unbound KS orbitals.
[e]The average absolute error with respect to the ''exact'' values is given in mhartrees.

TABLE VIII. Beryllium singlet excitation energies (in hartrees), uncertainties in the final digit in parentheses.

Transition	Expt.[a]	KS eigenvalues[b]	ALDA,full[c]	PT[d]	LB[e]	LDA[f]
$2s\rightarrow 2p$	0.193941	0.1327	0.1868	0.1989	0.1747(1)	0.1772(1)
$2s\rightarrow 3s$	0.249127	0.2444	0.2495	0.2556	0.2402(2)	0.2040(5)
$2s\rightarrow 3p$	0.274233	0.2694	0.2710	0.2741	0.2593(3)	
$2s\rightarrow 3d$	0.293556	0.2833	0.2778	0.2852	0.2669(3)	
$2s\rightarrow 4s$	0.297279	0.2959	0.2977(1)	0.2990		
$2s\rightarrow 4p$	0.306314	0.3046	0.3048(1)	0.3061		
$2s\rightarrow 4d$	0.313390	0.3098	0.3084(1)	0.3106		
$2s\rightarrow 5s$	0.315855	0.3153	0.3160(1)	0.3166		
Av. abs. error (mhartrees)[g]		11.0(3.9)	4.2(3.8)	3.2		

[a]The experimental excitation energies [75].

[b]Zeroth-order approximation provided by differences in KS eigenvalues.

[c]This work, ALDA results obtained by taking into account all bound and unbound KS orbitals.

[d]Values obtained by DFT perturbation theory [32].

[e]Van Leeuwen–Baerends potential [35]. The higher excitation energies are not given as they vary too much in different basis sets.

[f]The VWN parametrization is used [38]. Only the results for the transitions to bound virtual KS orbitals are given.

[g]The average absolute error with respect to the ''exact'' values is given in mhartrees, in parentheses the value for all but the for all but the first transition.

to increased basis set effects in the very low density region. The typical magnitude of the differences is a few millihartrees. For this reason we decided not to include those numbers in this and the following tables.

The LB results are much better already than the LDA potential. Due to the correct asymptotics, these Rydberg-like transitions are described reasonably well, with an average error of 17.4 millihartree (this should be compared to our results with the accurate xc potential, which yields an average error of 6.6 mhartree for these transitions).

The accurate potential results are better still. The average error of 4.2 mhartree gives a factor of 2.6 improvement with respect to the LB results, and a factor of 2.5 improvement with respect to the orbital energy differences. However, if the $2s\rightarrow 2p$ transition is disregarded (a very large correction to the orbital energy difference is needed for this transition), the ALDA results do not improve upon the orbital energy differences at all. This is entirely due to the $s\rightarrow d$ transitions, which are poorly treated by the ALDA kernel. Not only are the ALDA results for these transitions clearly worse than both the exact exchange-only results and the orbital energy differences, they even correct the orbital energy differences in the wrong direction. The results by Filippi *et al.* do provide a correction in the right direction, although by too small an amount.

On the other hand, the $s\rightarrow s$ and $s\rightarrow p$ transitions are treated satisfactorily by the ALDA kernel. The errors in the ALDA results for $s\rightarrow s$ transitions (0.4, 0.4, and 0.15 mhartree) are considerably lower than those for the $s\rightarrow p$ transitions (7.1, 3.2, and 1.5 mhartree), which in turn are superior to the $s\rightarrow d$ transition results with errors of 15.8 and 5.0 mhartree. The ALDA results for the $s\rightarrow s$ transitions are clearly better than the exact exchange results and the orbital energy differences, as was also the case for the singlet $s\rightarrow s$ transitions of helium in Table VII.

On the whole, the perturbative values obtained by Filippi *et al.* [32] are somewhat more accurate than our ALDA results here, with an average error of 3.2 mhartree. The quality of their results does not show the same variety in errors for the different types of transitions. It has already been observed by Petersilka and Gross [17] that the singlet spectrum is reproduced at least as well by the TDOEP kernel as by the ALDA kernel, while the ALDA kernel is to be preferred for triplet excitation energies.

The ALDA and exchange-only triplet energies for beryllium in Table IX provide corrections in the right direction with respect to the orbital energy differences for all transitions except the $2s\rightarrow 4p$ transition. The ALDA results, with an average absolute error of 2.7 mhartree, are clearly better than the exchange-only results (6.4 mhartree), which do not improve upon the orbital energy differences here (6.1 mhartree). As in the singlet case, the LB and LDA results are clearly worse.

In Table X the singlet-triplet splittings for beryllium are given. For the three lowest transitions, the ALDA splitting is clearly superior to the exchange-only splitting and can be considered very satisfactory. For the higher transitions, this is not the case anymore. The ALDA results for the $s\rightarrow d$ transitions are even qualitatively incorrect, as the wrong sign for the singlet-triplet splitting is predicted by the ALDA kernel. Although the exchange-only results by Filippi *et al.* [32] for these splittings are also not very impressive, they at least give the right sign. The wrong sign remains if one uses either only bound orbitals or the single pole approximation. If one uses only the exchange part of the ALDA kernel, the singlet-triplet splitting for the $2s\rightarrow 3d$ transition remains negative, but the right sign is predicted if one totally neglects the xc screening (only ''Coulomb'' screening).

TABLE IX. Beryllium triplet excitation energies (in hartrees), uncertainties in the final digit in parentheses.

Transition	Expt.[a]	KS eigenvalues[b]	ALDA,full[c]	PT[d]	LB[e]	LDA[f]
$2s\rightarrow 2p$	0.100153	0.1327	0.08885	0.0629	0.07665(1)	0.08675
$2s\rightarrow 3s$	0.237304	0.2444	0.2382	0.2331	0.2265(1)	0.2021(4)
$2s\rightarrow 3p$	0.267877	0.2694	0.2647	0.2640	0.2527(2)	
$2s\rightarrow 3d$	0.282744	0.2833	0.2802	0.2814	0.2694(2)	
$2s\rightarrow 4s$	0.293921	0.2959	0.2941	0.2928		
$2s\rightarrow 4p$	0.300487	0.3046	0.3030	0.3029		
$2s\rightarrow 4d$	0.309577	0.3098	0.3085	0.3089		
$2s\rightarrow 5s$	0.314429	0.3153	0.3145	0.3139		
Av. abs. error (mhartrees)[g]		6.1	2.7	6.4		

[a]The experimental excitation energies [75].
[b]Zeroth-order approximation provided by differences in KS eigenvalues.
[c]This work, ALDA results obtained by taking into account all bound and unbound KS orbitals.
[d]Values obtained by DFT perturbation theory [32].
[e]Van Leeuwen–Baerends potential [35]. The higher excitation energies are not given as they vary too much in different basis sets.
[f]The VWN parametrization is used [38]. Only the results for the transitions to bound virtual KS orbitals are given.
[g]The average absolute error with respect to the ''exact'' values is given in mhartrees.

We obtained similar inversions of the singlet and triplet levels for the $2s\rightarrow 4f$ transition in Be and the $s\rightarrow d$ and $s\rightarrow f$ transitions in helium. For these helium transitions, the absolute value of the splitting (which should be in the microhartree regime) is clearly overestimated as well, both in the SPA and in the full ALDA results. We do not presume that this is a basis set artifact, because it was reproduced in different basis sets of high quality. In the same basis sets, the approximation $f_{xc}=0$ (Coulomb screening only) does lead to positive values for all splittings. As the Coulomb-type matrix elements obtained in this way determine the TDOEP exchange-only results for He, we can actually calculate the results that would be obtained by Filippi *et al.* for these transitions, or by Petersilka *et al.* in their SPA-TDOEP results. In turns out that the TDOEP kernel correctly predicts positive singlet-triplet splittings for the $s\rightarrow d$ and $s\rightarrow f$ transitions in helium. Even higher quality calculations than the present ones would be required to see whether these splittings are also of the correct magnitude, although our results indicate that they probably will be.

TABLE X. Beryllium singlet-triplet splittings (in millihartrees), uncertainties in the final digit in parentheses.

Transition	Expt.[a]	ALDA, full[b]	PT[c]	LB[d]	LDA[e]
$2s\rightarrow 2p$	93.8	98.0	136	98.0(1)	90.4(1)
$2s\rightarrow 3s$	11.8	11.3	22.5	13.7(1)	2.3(1)
$2s\rightarrow 3p$	6.4	6.3	10.1	6.6(1)	
$2s\rightarrow 3d$	10.8	-2.4	3.8	$-2.5(1)$	
$2s\rightarrow 4s$	3.4	3.6	6.2		
$2s\rightarrow 4p$	5.8	1.8	3.2		
$2s\rightarrow 4d$	3.8	-0.1	1.7		
$2s\rightarrow 5s$	2.4	1.5	2.7		
Av. err. (mhartrees)		6.1	8.9		

[a]The experimental excitation energies [75].
[b]This work, ALDA results obtained by taking into account all bound and unbound KS orbitals.
[c]Values obtained by DFT perturbation theory [32].
[d]Van Leeuwen–Baerends potential [35]. The higher excitation energies are not given as they vary too much in different basis sets.
[e]The VWN parametrization is used [38]. Only the results for the transitions to bound virtual KS orbitals are given.

These SPA results can be understood from the SPA expression for the singlet-triplet splitting in Eq. (18). From that expression, it is clear that approximations for f_{xc} which are diagonal in spin space (such as the TDOEP and exchange-only ALDA kernels) yield no contribution to the singlet-triplet splitting in the SPA. Only the Coulomb term in Eq. (18) remains in that case. For this reason, it should not be very surprising that the ALDA results for the splittings are usually better than the TDOEP kernel results. This expression also explains why only the ALDA xc kernel can give rise to negative SPA singlet-triplet splittings. Apparently, the correlation part of the ALDA kernel, based on the homogeneous electron gas, is too crude to provide an accurate correction for this very subtle and small effect for these transitions. In short, we can state that although the correlation part of the ALDA kernel in general yields improved results with respect to the exchange-only approximations, the negative singlet-triplet splittings to which it gives rise show that it still needs to be improved upon.

The LB results show that the singlet-triplet splittings are more sensitive to the xc kernel than to details of the xc potential, because they are very similar to the ALDA results with the accurate potential. The LDA results, on the other hand, show that the xc potential should at least possess the correct asymptotic behavior in order to obtain reliable singlet-triplet splittings for the higher-lying excitations. Only the LDA result for the first splitting is qualitatively correct.

TABLE XI. Molecular polarizabilities with LDA, LB, and semi-accurate potential.

Molecule	LDA	LB	Accurate v_{xc}[a]	Acc.-Expt.[b]
H_2	5.9	5.61	5.16	5.1816[c]
N_2	12.27	11.46	11.68	11.74
HF	6.20	5.31	5.49	5.52[d]
HCl	18.63	17.86	17.25	17.39
H_2O	10.53	9.20	9.45	9.64
CO	13.87	12.62	12.86	13.08
Av. err.	+8.8%	−0.6%	−1.0%	
Av. abs. err.	+8.8%	3.6%	−1.0%	

[a]Results obtained with large GTO basis sets for the CI. The difference in the polarizability by using another large augmented GTO basis set is smaller than 1%, typically a few tenths of a percent.
[b]Benchmark theoretical or experimental results.
[c]Vibrationless theoretical value.
[d]Vibrationless estimate.

D. Molecular polarizability results

We have performed polarizability calculations using xc potentials constructed from (MR)SDCI densities, as has been pointed out earlier. The results for the static average polarizabilities of some small molecules are given in Table XI. We used the experimental equilibrium bond distances of 1.4 bohr for H_2 (0.7408 Å), 0.917 Å for HF, 1.2746 Å for HCl, 1.12832 Å for CO, 1.09768 Å for N_2, and 0.957 Å for the H—O distance in H_2O, with a H—O—H angle of 104.5°.

As usual, the LDA results are clearly and invariably too high (on average 8.8%). The LB results are much better. They do not show a systematic error (the average error is only 0.6%), and the average absolute error (3.6%) is considerably lower than for the LDA results (8.8%). The results with the accurate potentials are much better still. The average absolute error reduces by almost a factor of 4 to 1.0% with respect to the LB results. This is a strong indication that improved models for v_{xc} will considerably improve molecular polarizability results. The results with the accurate potential are invariably too low with respect to the experimental or vibrationless theoretical results. Several reasons can be given for this. The most obvious one is that the CI results for the polarizabilities (which we obtained from finite field CI calculations, using the same type of CI that generated the density from which the ''accurate'' v_{xc} was constructed) are also invariably too low. In most cases the underestimation was even more than the result with the accurate potential; for example, we obtained from the finite field CI calculations a polarizability of 5.185 for H_2, 16.97 for HCl, and 9.20 for H_2O (where the accurate potential results were 5.16, 17.25, and 9.45, respectively).

This implies that either the basis sets we used in the CI calculations were not large enough or the level of CI (which was SD) was insufficiently high. We expect both factors to contribute. As far as the level of correlation is concerned, it is known from coupled-cluster response calculations that CCSD(T) results are often clearly better than CCSD or CISD results. In the basis sets we used, one or more sets of augmenting functions were added, and we obtained Hartree-Fock results for the polarizabilities which were close to the basis-set limit values. This does not imply that these basis sets were sufficiently large for the correlated calculations, however.

One might furthermore suspect our construction scheme for the potential to influence the polarizability results artificially. This could lead to a small (possibly systematic) error in either direction. A final suggestion that the remaining 1% error is due to the intrinsic errors of the xc kernel f_{xc} cannot be dismissed, although it is much too early on the basis of this evidence to jump to such a conclusion. Finally, a comparison of our LDA values to the basis set free values obtained by Dickson and Becke [63] shows that our basis sets in the DFT calculation are sufficiently large.

It should be emphasized that we do not suggest the present approach as a practical method for calculating polarizabilities. We have merely tried to indicate that an accurate future model for the xc potential will yield considerable improvements in molecular polarizabilities as well. Similar preliminary calculations on excitation energies and hyperpolarizability have not led to such a clear picture, however. It would be desirable to repeat a similar molecular study using a higher level correlated method than the present one, preferably in a fully numerical program, or in a large STO basis set (although in the latter case one has to make sure that the density in the outer region decays correctly). Such a study would allow more definite statements to be made.

V. CONCLUSIONS AND FUTURE DIRECTIONS

We have performed accurate atomic calculations using accurate xc potentials on excitation energies and polarizabilities of three small atoms: He, Be, and Ne. Our results show that important improvements with respect to calculations using the LDA potential or LB potential are obtained. The use of an accurate xc potential removes the larger part of the discrepancy with respect to the experimental values. The remaining discrepancies are due to deficiencies in the ALDA xc kernel. Our results show that the ALDA kernel is at least comparable in quality to the exchange-only TDOEP kernel and that taking into account ''continuum contributions'' has a positive effect on the calculated excitation energies.

We believe that the major deficiencies in the xc kernels are still in the spatial part, not in the frequency dependence. Major improvements may come from a TDOEP kernel, which includes accurate correlation contributions. This correlation contribution is clearly important in the results for the singlet-triplet splittings. Further improvement should come from improved modeling of the frequency dependence of the kernel.

The benefit of more refined approximations for the xc kernel will be useful only in combination with improved xc potentials. At the very least, these potentials should be self-interaction free, or, in other words, possess the correct asymptotic behavior. Such potentials can be constructed by either adding a (semiempirical) correction to a usual xc potential as in the LB potential [35], or by using OEP potentials in the Krieger-Li-Iafrate [64] (KLI) approximation [65–67]. Such an xc potential has to yield accurate predictions for the

experimental ionization potential in order to improve upon existing approximate xc potentials.

ACKNOWLEDGMENTS

We are grateful to Professor Dr. Umrigar [31,30] for providing the accurate xc potentials for He and Be, and to the authors of Ref. [49,32] for making their work available prior to publication. We thank Martin Petersilka for sending his work prior to publication and for many very useful discussions. S.v.G. gratefully acknowledges financial support from the Netherlands Organization for Scientific Research (NWO) through its foundations SON and NCF.

[1] H. Sekino and J. Bartlett, Chem. Phys. Lett. **234**, 87 (1995).
[2] C. Hättig, O. Christiansen, H. Koch, and P. Jørgensen, Chem. Phys. Lett. **269**, 428 (1997).
[3] J. Olsen and P. Jørgensen, in *Modern Electronic Structure Theory*, edited by D. R. Yarkony, Advanced Series in Physical Chemistry Vol. 2 (World Scientific, Singapore, 1995), p. 857.
[4] J. E. Rice and N. C. Handy, J. Chem. Phys. **94**, 4959 (1991).
[5] F. Aiga and R. Itoh, Chem. Phys. Lett. **251**, 372 (1996).
[6] C. Hättig and B. A. Hess, Chem. Phys. Lett. **233**, 359 (1995).
[7] C. Hättig and B. A. Hess, J. Chem. Phys. **105**, 9948 (1996).
[8] A. Zangwill and P. Soven, Phys. Rev. A **21**, 1561 (1980).
[9] E. Runge and E. K. U. Gross, Phys. Rev. Lett. **52**, 997 (1984).
[10] E. K. U. Gross, J. F. Dobson, and M. Petersilka, in *Density Functional Theory*, edited by R.F. Nalewajski, Topics in Current Chemistry (Springer, Heidelberg, 1996) .
[11] Z. H. Levine and P. Soven, Phys. Rev. A **29**, 625 (1984).
[12] S. J. A. van Gisbergen, V. P. Osinga, O. V. Gritsenko, R. van Leeuwen, J. G. Snijders, and E. J. Baerends, J. Chem. Phys. **105**, 3142 (1996).
[13] C. Jamorski, M. E. Casida, and D. R. Salahub, J. Chem. Phys. **104**, 5134 (1996).
[14] V. P. Osinga, S. J. A. van Gisbergen, J. G. Snijders, and E. J. Baerends, J. Chem. Phys. **106**, 5091 (1997).
[15] U. Hohm, D. Goebel, and S. Grimme, Chem. Phys. Lett. **272**, 1059 (1997).
[16] M. Petersilka, U. J. Gossmann, and E. K. U. Gross, Phys. Rev. Lett. **76**, 1212 (1996).
[17] M. Petersilka and E. K. U. Gross, Int. J. Quantum Chem. Quantum Biol. Symp. **30**, 181 (1996).
[18] M. Petersilka, U. J. Gossmann, and E. K. U. Gross, in *Proceedings of the Brisbane Workshop on Electron Density Functional Theory*, edited by J. Dobson, G. Vignale, and M. P. Das (Plenum, New York, 1997).
[19] M. E. Casida, in *Recent Advances in Density-Functional Methods*, edited by D. P. Chong (World Scientific, Singapore, 1995), p. 155.
[20] M. E. Casida, in *Recent Developments and Applications of Modern Density Functional Theory*, edited by J. M. Seminario (Elsevier, Amsterdam, 1996).
[21] R. Bauernschmitt and R. Ahlrichs, Chem. Phys. Lett. **256**, 454 (1996).
[22] R. Bauernschmitt, M. Häser, O. Treutler, and R. Ahlrichs, Chem. Phys. Lett. **264**, 573 (1997).
[23] F. Kootstra, internal report, Vrije Universiteit, Amsterdam, 1997 (unpublished).
[24] S. J. A. van Gisbergen, J. G. Snijders, and E. J. Baerends, Phys. Rev. Lett. **78**, 3097 (1997).
[25] S. J. A. van Gisbergen, J. G. Snijders, and E. J. Baerends, J. Chem. Phys. **103**, 9347 (1995).
[26] S. J. A. van Gisbergen, J. G. Snijders, and E. J. Baerends, Chem. Phys. Lett. **259**, 599 (1996).
[27] P. R. T. Schipper, O. V. Gritsenko, and E. J. Baerends, Theor. Chem. Acc. **98**, 16 (1997).
[28] R. O. Esquivel and A. V. Bunge, Int. J. Quantum Chem. **32**, 295 (1987).
[29] A. V. Bunge and R. O. Esquivel, Phys. Rev. A **34**, 853 (1986).
[30] C. J. Umrigar and X. Gonze, Phys. Rev. A **50**, 3827 (1994).
[31] C. J. Umrigar and X. Gonze, in *High Performance Computing and Its Application to the Physical Sciences*, Proceedings of the Mardi Gras '93 Conference, edited by D. A. Browne *et al.* (World Scientific, Singapore, 1993); (unpublished).
[32] C. Filippi, C. J. Umrigar, and X. Gonze, J. Chem. Phys. **107**, 9994 (1997).
[33] P. Hohenberg and W. Kohn, Phys. Rev. **136**, B864 (1964).
[34] W. Kohn and L. J. Sham, Phys. Rev. **140**, A1133 (1965).
[35] R. van Leeuwen and E. J. Baerends, Phys. Rev. A **49**, 2421 (1994).
[36] S. M. Colwell, C. W. Murray, N. C. Handy, and R. D. Amos, Chem. Phys. Lett. **210**, 261 (1993).
[37] S. J. A. van Gisbergen, J. G. Snijders, and E. J. Baerends (unpublished). .
[38] S. H. Vosko, L. Wilk, and M. Nusair, Can. J. Phys. **58**, 1200 (1980).
[39] E. K. U. Gross and W. Kohn, Phys. Rev. Lett. **55**, 2850 (1985).
[40] E. K. U. Gross and W. Kohn, Phys. Rev. Lett. **57**, 923 (1986).
[41] N. Iwamoto and E. K. U. Gross, Phys. Rev. B **35**, 3003 (1987).
[42] E. K. U. Gross and W. Kohn, Adv. Quantum Chem. **21**, 255 (1990).
[43] G. D. Mahan and K. R. Subbaswamy, *Local Density Theory of Polarizability* (Plenum, New York, 1990).
[44] E. J. Baerends, D. E. Ellis, and P. Ros, Chem. Phys. **2**, 41 (1973).
[45] G. te Velde and E. J. Baerends, J. Comput. Phys. **99**, 84 (1992).
[46] C. F. Guerra, O. Visser, J. G. Snijders, G. te Velde, and E. J. Baerends, in *Methods and Techniques in Computational Chemistry*, edited by E. Clementi and G. Corongiu (STEF, Cagliari, Italy, 1995), p. 305.
[47] RESPONSE, extension of the ADF program for linear and nonlinear response calculations, by S. J. A. van Gisbergen, J. G. Snijders and E. J. Baerends, with contributions by J. A. Groeneveld, F. Kootstra, and V. P. Osinga.
[48] http://tc.chem.vu.nl/~vgisberg/basissets.html.
[49] A. Savin, C. J. Umrigar, and X. Gonze (unpublished).
[50] V. R. Saunders and J. H. van Lenthe, Mol. Phys. **48**, 923 (1983).
[51] A. Savin, H. Stoll, and H. Preuss, Theor. Chim. Acta **70**, 407 (1986).
[52] D. E. Woon and T. H. Dunning, Jr., J. Chem. Phys. **100**, 2975 (1994).

[53] O. V. Gritsenko, R. van Leeuwen, and E. J. Baerends, Phys. Rev. A **52**, 1870 (1995).
[54] G. D. Mahan, Phys. Rev. A **22**, 1780 (1980).
[55] O. Gunnarsson and B. I. Lundqvist, Phys. Rev. B **13**, 4274 (1976).
[56] S. A. C. McDowell, R. D. Amos, and N. C. Handy, Chem. Phys. Lett. **235**, 1 (1995).
[57] D. M. Bishop and J. Pipin, Int. J. Quantum Chem. **45**, 349 (1993).
[58] P. J. Leonard, At. Data Nucl. Data Tables **14**, 22 (1974).
[59] G. Senatore and K. R. Subbaswamy, Phys. Rev. A **35**, 2440 (1987).
[60] A. Görling and M. Levy, Phys. Rev. B **47**, 13 105 (1993).
[61] A. Görling and M. Levy, Int. J. Quantum Chem. Quantum Biol. Symp. **29**, 93 (1995).
[62] M. Petersilka (private communication).
[63] R. M. Dickson and A. D. Becke, J. Phys. Chem. **100**, 16 105 (1996).
[64] J. B. Krieger, J. Chen, Y. Li, and G. J. Iafrate, Int. J. Quantum Chem. Quantum Biol. Symp. **29**, 79 (1995).
[65] T. Grabo and E. K. U. Gross, Chem. Phys. Lett. **240**, 141 (1995).
[66] T. Grabo and E. K. U. Gross, Int. J. Quantum Chem. **64**, 95 (1997).
[67] X.-M. Tong and S.-I. Chu, Phys. Rev. A **55**, 3406 (1997).
[68] D. Tunega, J. Noga, and W. Klopper, Chem. Phys. Lett. **269**, 435 (1997).
[69] A. J. Thakkar, Phys. Rev. A **40**, 1130 (1989).
[70] G. Maroulis and A. J. Thakkar, J. Phys. B **21**, 3819 (1988).
[71] P. R. Taylor, T. J. Lee, J. E. Rice, and J. Almlöf, Chem. Phys. Lett. **163**, 359 (1989).
[72] A. J. Thakkar, H. Hettema, and P. E. S. Wormer, J. Chem. Phys. **97**, 3252 (1992).
[73] G. W. F. Drake, in *Atomic, Molecular, and Optical Physics Handbook*, edited by G. W. F. Drake (AIP Press, Woodbury, NY, 1996), p. 154 .
[74] A. Kono and S. Hattori, Phys. Rev. A **29**, 2981 (1984).
[75] S. Bashkin and J. A. Stoner, Jr., *Atomic Energy Levels and Grotrian Diagrams 1* (North-Holland, Amsterdam, 1975).